

# Impact of dissipative effects on the macroscopic evolution of a Vlasov system

L. Galeotti, F. Califano

*Physics Dept., University of Pisa and INFN, Pisa, Italy*

(Dated: July 17, 2018)

Numerical diffusion is introduced by any numerical scheme as soon as small scales fluctuations, generated during the dynamical evolution of a collisionless plasma, become comparable to the grid size. Here we investigate the role of numerical dissipation in collisionless plasma simulations by studying the non linear regime of the two stream instability. We show that the long time evolution of the Vlasov - Poisson system can be affected by the used algorithm.

PACS numbers: 52.65.Ff, 52.35.Qz, 52.35.Fp, 52.35.Mw

Many space and laboratory plasmas can be considered as weakly collisional since the collisional frequency is smaller than all the other frequencies, as for example the plasma frequency. In other words, for these plasmas, the mean free path of the particles is (much) longer than all the other characteristic length scales of the plasma and, sometimes, even larger than the dimension of the plasma itself. At first approximations such plasmas can be considered as collisionless and their dynamics can be well represented using a Hamiltonian description. This approach is based on the idea that the dissipative scale (for example in numerical simulations the grid size) is much smaller than any macroscopic physical length scale of the system, so that dissipation has no feedback on the macroscopic asymptotic evolution of the system.

Numerical simulations based on non collisional models must necessarily face with the small scales generation problem during the dynamical evolution of the system; indeed, when the typical length scales of the fluctuations become comparable to the grid size, numerical dissipation comes into play leading the system to violate the conservation constraints of Hamiltonian dynamics and to reconnect close isolines of the distribution function (d.f.). This process, formally forbidden, is very well highlighted by the time evolutions of the system invariants  $N_i = \int f^i dx dv$   $i = 1, 2, ..$  and by the "entropy"  $S = - \int f \ln(f) dx dv$  (here  $f$  is the d.f.), showing sudden variations when closed vortices are formed in phase space as a consequence of particle trapping.

In this paper, through numerical studies of a non-linear regime of a collisionless plasma, we discuss the role of artificial dissipation introduced by a numerical scheme on the plasma dynamics, influencing the final Vlasov evolution of the system even if the grid size is much shorter than any physical relevant scale length. The dynamical non linear evolution we chose for our numerical simulations is the well-known two stream instability. In this case, dissipation allow for the formation of coherent macroscopic structures in phase space (vortices).

Since the non-linear dynamics of the two stream instability is substantially driven by kinetic effects, especially concerning the saturation phase where particle trapping play a crucial role, a kinetic approach is nec-

essary. This can be done using Vlasov equation, which replaces Coulomb interactions between charged particles with a mean electromagnetic field. This field is determined self-consistently through the particle distribution function by Maxwell and Poisson equations. Since the two stream instability is driven by purely electrostatic mechanisms, we limit our study to the solution of the 1D-1V Vlasov - Poisson system of equations:

$$\frac{\partial f_a}{\partial t} + v \frac{\partial f_a}{\partial x} - \frac{m_e}{m_a} \frac{\partial \phi}{\partial x} \frac{\partial f_a}{\partial v} = 0; \quad a = e, p \quad (1)$$

$$\frac{\partial^2 \phi}{\partial x^2} = \int (f_e - f_p) dv; \quad E = -\frac{\partial \phi}{\partial x} \quad (2)$$

In these equations and in the rest of this paper, time  $t$  is normalized to the inverse of the electron plasma frequency  $\omega_{pe}$ , velocities  $v_e$  and  $v_p$  to the electronic thermal velocity  $v_{th,e}$ , electron and proton distribution functions,  $f_e$  and  $f_p$ , to the equilibrium particle density  $n_0$ , lengths to the Debye length  $\lambda_D = v_{th,e}/\omega_{pe}$  and the electric field  $E$  to  $m_e v_{th,e} \omega_{pe}/e$ . As mentioned above, the dynamics described by this system of equations is characterized by the absence of collisions; hence, from a numerical point of view, the choice of an algorithm that is capable to conserve better than possible the invariants of the system is crucial. Our numerical scheme is based on the splitting scheme of Cheng and Knorr, 1976, [1] for the solution of the Vlasov equation; therefore, the problem is mainly reduced to an interpolation problem for the distribution function. Here we compare three well known interpolation algorithms, namely the Van Leer method at second and third order [2] (at which, in the text, we'll refer as VL2 and VL3) and the Spline method [3] (a third order method). The Poisson equation is solved, at every time step, by spectral methods (i.e. fast Fourier Transform technique); in particular, we calculate the plasma density by integrating the electron distribution functions in velocity.

We made the two stream instability runs for the three simulation algorithms (VL2, VL3 and Spline, runs A, B and C, respectively) using the same identical parameters

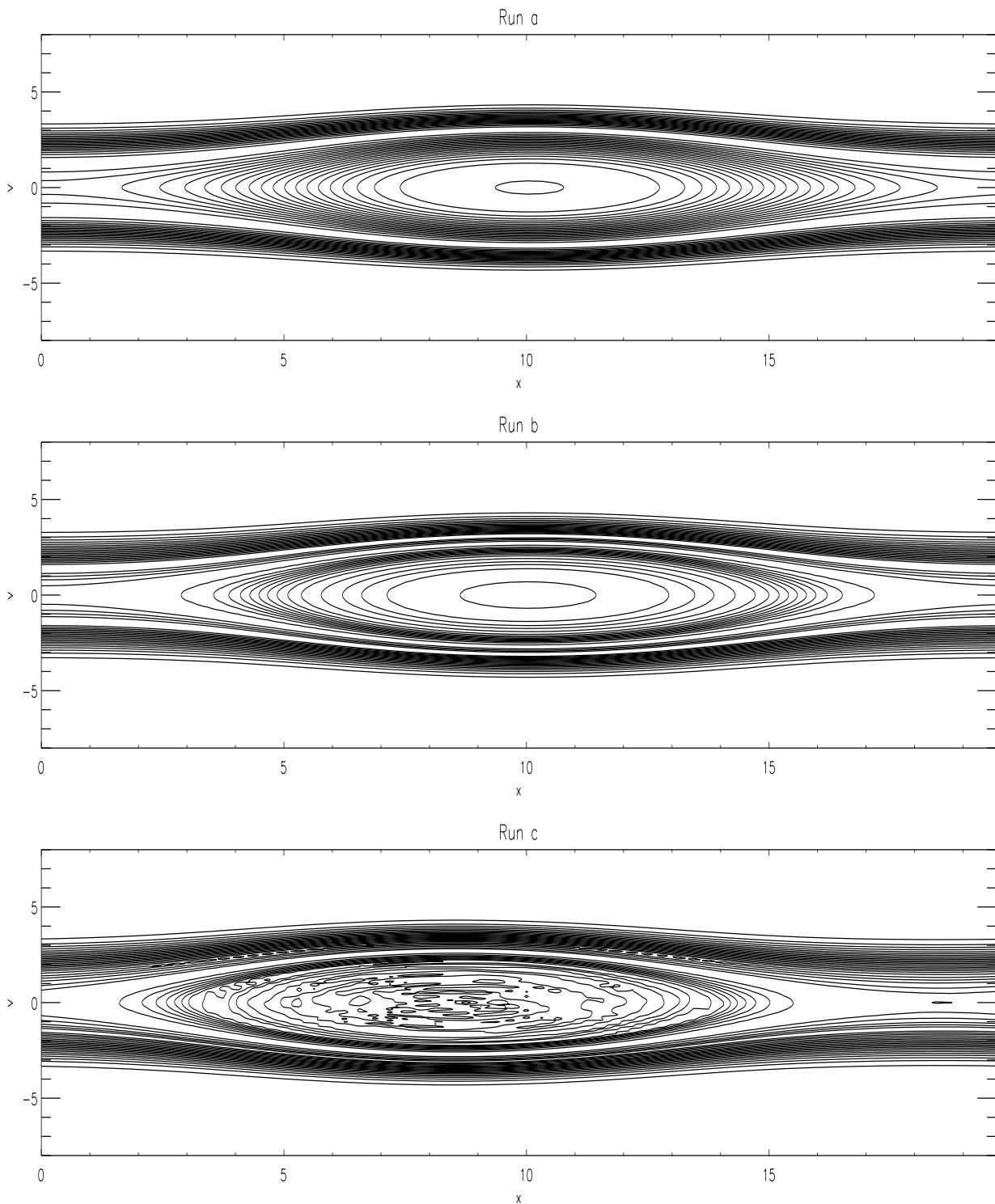


FIG. 1: Electron distribution functions in phase space at time  $t=1200$  of, top to bottom, the VL2, VL3 and Spline algorithm, runs A, B and C, respectively.

(however, we recall that the CPU time for the three algorithms is not equal). The simulation box is  $L_x = 20\lambda_D$  in space and the velocity interval is  $-v_{max} \leq v \leq v_{max}$ , with  $v_{max} = 5v_{th,e}$ . We use  $N_x = 128$  points in space

and  $N_v = 501$  in velocity, corresponding to a phase space grid resolution of  $dx = 0.16$  and  $dv = 0.02$ . Other parameters are: amplitude of the initial random perturbation of  $\epsilon = 0.0001$ ;  $dt = 0.0003\omega_{pe}^{-1}$ , total simulation time

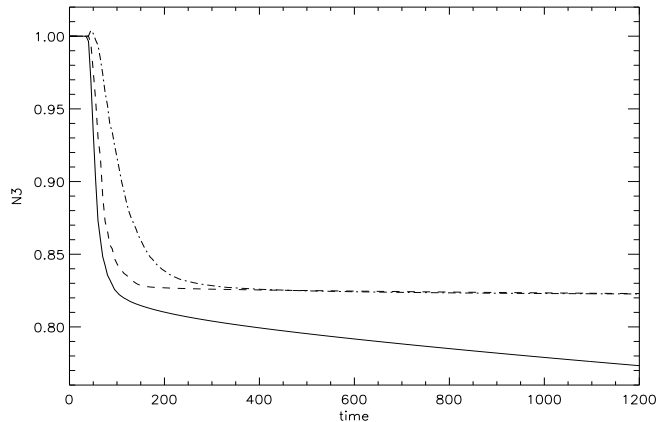


FIG. 2: The time evolution of the third invariant. The continuous, dashed and dot-dashed lines correspond to run A to C, respectively.

equal to  $1200 \omega_{pe}^{-1}$ ; modulo of mean velocity of the two initial electron streams ( $u_0$ ) equal to  $2 v_{th,e}$ . The initial electron distribution function we use is

$$f_e(x, v_e, 0) = f_M(v_e) \left[ 1 + \epsilon \sum_{k=1}^{30} \cos(kx + \phi_k) \right] \quad (3)$$

$$f_M = \frac{1}{\sqrt{2\pi} v_{th}} (e^{-((v_e - v_0)^2 / 2v_{th}^2)} + e^{-((v_e + v_0)^2 / 2v_{th}^2)}) \quad (4)$$

In Fig. 1 we show the phase space vortices (same contour levels) generated by the evolution of the instability. There is an initial good agreement among the results of the three algorithms: the vortex appears at the same time for all methods and is displaced in the same position. On the other hand, we observe that the Spline vortex (run C) propagates with a different velocity with respect to the vortex obtained with VL2 and VL3 (runs A, B) method. Furthermore, the spatial structure of the VL2 vortex is significantly different from that of the vortices obtained with the other two algorithms.

By looking at the behavior of the  $N_3$  invariant, Fig. 2, we see in all cases a sudden decrease of the invariant as soon as the vortices start to form. This is a consequence of the d.f. lines reconnection processes at the grid scale length where the algorithm is forced to introduce some artificial dissipation eventually leading to the closure of the particle orbits (i.e. vortices) contrary to the Hamiltonian character of the equations. We note that both VL3 and Spline invariants tend to a (equal) constant asymptotic value, while VL2 continues to smoothly decrease, meaning that the numerical resolution for the VL2 algorithm must be increased (even if both  $dx$  and  $dv$  are much shorter than the vortex dimension), as also shown by the time evolution of the total energy variations of the system in Fig. 3 where we plot the evolution of the normalized energy variations defined as

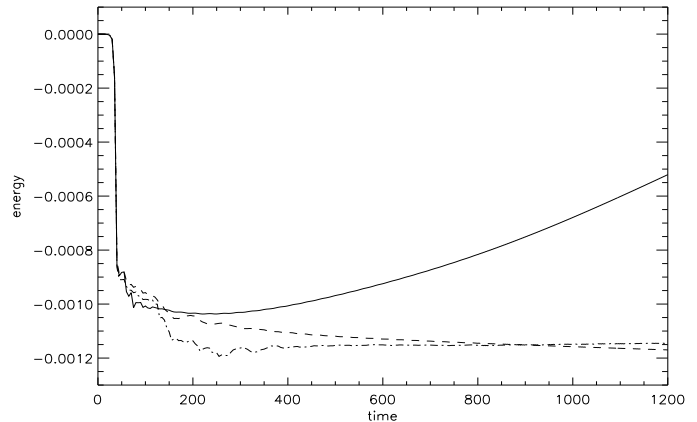


FIG. 3: The time evolution of  $\delta E$  (same line style as in fig. 1).

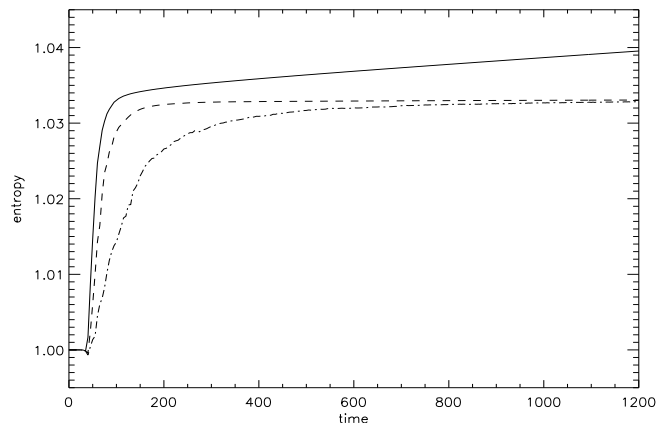


FIG. 4: The time evolution of the entropy (same line style as in fig. 2).

$\delta E = (E_{tot} - E_{tot}(t=0)) / E_{tot}(t=0)$ . Indeed, we see that after the phase space vortex formation, the energy variation for VL3 and Spline algorithms becomes nearly constant, while for VL2 begins to monotonically increase. In Fig. 4 we show the time evolution of the entropy. We again observe a strong variation of entropy during the vortex formation phase for all three algorithms while in the asymptotic limit the entropy becomes nearly constant for both VL3 and Spline, while continues to increase for VL2. The uncorrect behavior of the VL2 method with respect to VL3 and Spline is the consequence of the fact that VL2 method is a lower order scheme. We underline that VL2 is however a II order scheme (II order schemes are often used in collisionless simulations) and that the grid spacing,  $dx \ll \lambda_D$  and  $dv \ll v_{th,e}$ , seems to be adequate for correctly describing the formation of a coherent structure much larger than  $dx \times dv$ . To clarify this point, we made a number of other runs with different numerical accuracy, corresponding to different computational times. For the algorithms here used, we know that for

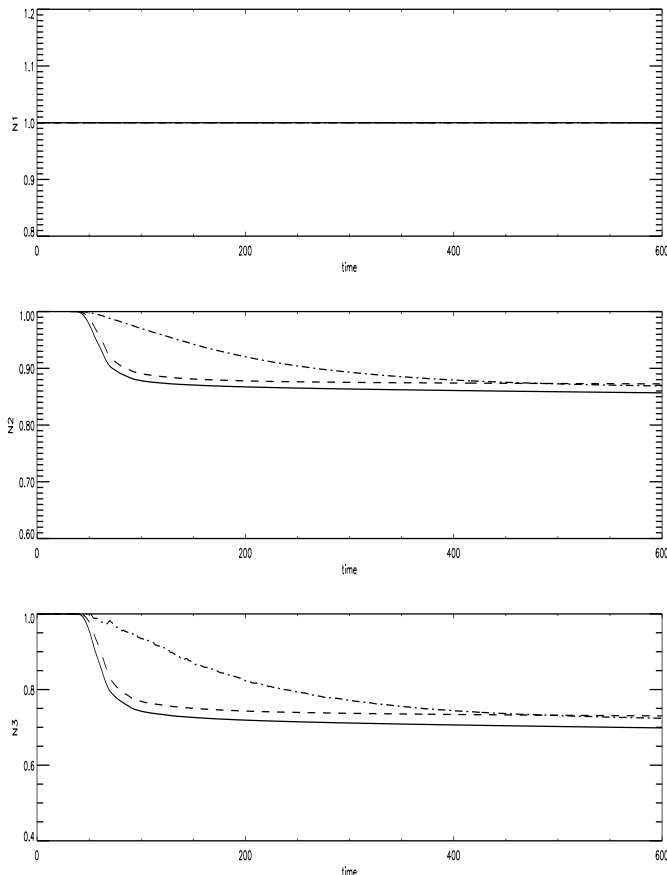


FIG. 5: The time evolution of the invariants  $N_1$  (total charge density),  $N_2$  and  $N_3$ . The continuous, dashed and dot-dashed lines correspond to runs D, E and F made with the VL2, VL3 and Spline algorithm, respectively.

the same grid spacing the computational CPU time scales as:

$$\tau_{VL3} = \frac{3}{2} \tau_{VL2}, \quad \tau_{Spline} = 3\tau_{VL2} \quad (5)$$

where  $\tau_{VL2}$ ,  $\tau_{VL3}$  and  $\tau_{Spline}$  are the computational time for VL2, VL3 and Spline, respectively. The criterion we

used is to take a numerical accuracy for the three algorithms corresponding to the same computational time. We made the new runs by using all the same parameters of the previous runs, but with  $L_x = 30$  and  $v_{max} = 15v_{th,e}$ . The numerical mesh are:  $N_x=300$  and  $N_v=601$  for VL2 (run D),  $N_x=200$  and  $N_v=401$  for VL3 (run E) and  $N_x = 100$  and  $N_v = 201$  (run F) for Spline. We now found that the energy variation is now asymptotically constant for all methods. However, even if VL2 has a better resolution with respect to the other two methods, invariants decrease more than in VL3 or Spline. So, even at parity of computational time conditions, the fact that VL3 and Spline are third order methods while VL2 is a second order one has a relevant effect on the invariants. Finally, VL3 and Spline have different trends for invariants, but the same asymptotic values.

In conclusion, choosing a numerical algorithm means to select a determined quantity of artificial dissipation. This means that, even if the grid length scales are by far the shorter length scales of the system, the final state of the system can be affected by the kind of algorithm we have used. Furthermore, even by performing very accurate simulations, i.e. grid scales sufficiently short to have a "correct" long time behavior of the energy and the invariants, the long time nonlinear dynamics can be significantly different, in particular when more "turbulent" systems are studied (for example if some external forcing continues to inject energy during the nonlinear regime).

This work was supported, in part, by MURST. Laura Galeotti is pleased to acknowledge the INFN Parallel Computing Initiative for supporting her doctoral fellowship at Pisa University and for giving the access to computing facilities.

- 
- [1] C.Z.Cheng and G.Knorr, J. Comput. Phys. **22**, 330 (1976);
  - [2] A.Mangeney, F.Califano, C.Cavazzoni and P.Travnicek, J. Comput. Phys. **179**, 495 (2002);
  - [3] M.M.Shoucri and R.R.Gagn, J. Comput. Phys. **24**, 445 (1977);